that the last term in (29) and the last term in (31) contain the expressions $Y_{\pm}(x)$.

References

[1] Fan, D. N. and Ludford, G. S. S., "Correct Formulation of Airfoil Problems in Magnetoaerodynamics," *AIAA Journal*, Vol. 6, No. 1, Jan. 1968, pp. 167–169.

[2] Bhutani, O. P. and Nanda, K. D., "A General Theory of Thin Airfoils in Nonequilibrium Magnetogasdynamics. Part II: Transverse Magnetic Field," *AIAA Journal*, Vol. 6, No. 11, Nov. 1968, pp. 2122–2124.

[3] Dragos, L. "Theory of Thin Airfoils in Magnetoaerodynamics," *AIAA Journal*, Vol. 2, No. 7, July 1964, pp. 1223–1229.

[4] Dragos, L., "Reply by Author to P. Grenberg," *AIAA Journal*, Vol. 5, No. 7, July 1967, pp. 1367–1370.

[5] Guelfand, J. M. and Shilov, G. E., *Generalized Functions I*, Fizmatghiz, Moscow, 1958.

[6] Iacob, C., *Introduction Mathématique a la Mécanique des Fluides*, Bucarest E'ditions de l' Academie de la République Populaire Roumaine, Gauthier-Villars, Paris, 1959.

Bending of a Beam Made of a Fiber-Reinforced Viscoelastic Material

R. Ray Nachlinger* and J. R. Leininger†
University of Houston, Houston, Texas

Introduction

Due to their high strength and low weight, there has been a great increase in the use of fiber-reinforced materials in the past few years. Many of these materials consist of high-strength fibers imbedded in a matrix of a viscoelastic material. The long, thin fibers make the resulting composite material much stronger than the matrix alone in tension; but when the composite is compressed, the fibers buckle and a larger portion of the load is carried by the matrix. The net result of this effect is that if one has a composite with thin, long fibers, the material will behave essentially as an elastic material in tension and as a viscoelastic material in compression.

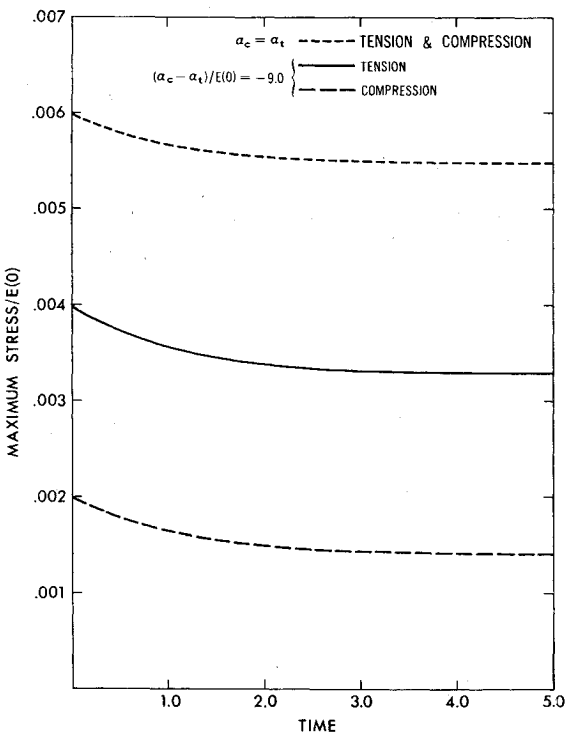

Fig. 1 Maximum stress vs time, constant radius of curvature, $R = 1000$.

This Note is an investigation of the bending of a beam made of the type of material previously discussed. The analysis that is carried out is for the case of a beam that is subjected to pure moments. The results of this analysis are quite surprising. They show that the maximum stress in the beam can be 50% greater than that predicted if the material is assumed to have the same modulus in both tension and compression.

Development of the Equations

The material from which the fiber-reinforced material is made is assumed to have a stress-strain relation given by

$$\sigma(t) = [\alpha + E(0)]\epsilon(t) + \int_0^t \dot{E}(\tau)\epsilon(t - \tau)d\tau \qquad (1)$$

where $E(t)$ is the relaxation function of the matrix and α takes into account the added stiffness due to the fibers. This relation assumes a rigid bond between the matrix and the fibers. Since the fibers will buckle in compression, α will be smaller when the material is in compression than when it is in tension. Thus, α is taken to be

$$\alpha = \begin{cases} \alpha t & \epsilon > 0 \\ \alpha c & \epsilon < 0 \end{cases} \qquad (2)$$

For the bending of a beam, the relevant equilibrium equations are

$$\int_A \sigma dA = 0, \int_A \sigma y dA = -M \qquad (3)$$

where y is measured from the neutral axis. The usual strain-curvature assumption will also be made, i. e.,

$$\epsilon = -y/\rho \qquad (4)$$

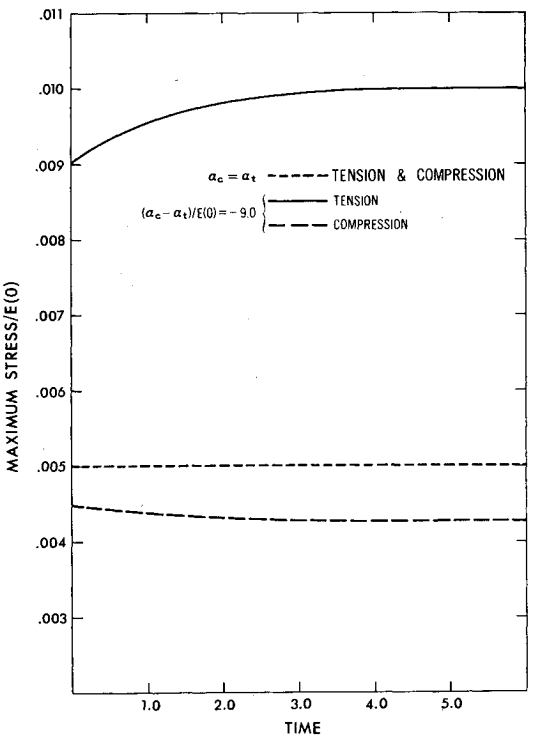

Fig. 2 Maximum stress vs time; $M/E(0) = 0.001$, $(\alpha_c - \alpha_t)/E(0) = -9.0$.

Received April 1, 1969.

* Assistant Professor, Department of Mechanical Engineering.
† Department of Mechanical Engineering.

where ρ is the radius of curvature.

The beam will be taken to be of rectangular cross section with a depth of b and a height of h. The distance from the bottom of the beam to the neutral axis will be taken to be c.

If Eqs. (1–4) are combined, the following relations result for the curvature and the location of the neutral axis:

$$\int_{-c}^{0} \alpha t \frac{y}{\rho(t)}\,dy + \int_{0}^{h-c} \alpha c \frac{y}{\rho(t)}\,dy + \int_{0}^{h-c} \left[E(0) \times \frac{y}{\rho(t)} + \int_{0}^{t} \frac{y}{\rho(t-\tau)} \dot{E}(\tau)d\tau\right] dy = 0 \tag{5}$$

$$\int_{-c}^{0} \alpha t \frac{y^2}{\rho(t)}\,dy + \int_{0}^{h-c} \alpha c \frac{y^2}{\rho(t)}\,dy + \int_{-c}^{h-c} \left[E(0) \times \frac{y^2}{\rho(t)} + \int_{0}^{t} \frac{y^2}{\rho(t-\tau)} \dot{E}(\tau)d\tau\right] = \frac{M(t)}{b}$$

After the spatial integration is carried out, Eqs. (5) become

$$\frac{c^2(t)}{\rho(t)}[\alpha c - \alpha t] + \left[\frac{\alpha c}{\rho(t)} + \frac{E(0)}{\rho(t)} + \int_{0}^{t} \frac{\dot{E}(\tau)}{\rho(t-\tau)}\,d\tau\right][h - 2hc(t)] = 0 \tag{6}$$

$$\frac{c^3(t)}{\rho(t)}[\alpha c - \alpha t] + \left[\frac{\alpha c}{\rho(t)} + \frac{E(0)}{\rho(t)} + \int_{0}^{t} \frac{\dot{E}(\tau)}{\rho(t-\tau)}\,d\tau\right][h^3 - 3h^2c(t) + 3hc^2(t)] = 3M(t)$$

After Eqs. (6) are solved for $c(t)$ and $\rho(t)$, Eqs. (1, 2, and 4) can be used to obtain the stresses.

If the beam is subjected to a constant radius of curvature, $\rho(t) = k$, Eqs. (6) can be solved analytically for $c(t)$ and $M(t)$. Figure 1 shows the stresses resulting from such a deformation for the cases $\alpha c \neq \alpha t$ and $\alpha c = \alpha t$. These results are not very interesting since the stresses obtained from the former are less than the latter. Thus if a design is based on the simpler analysis of assuming $\alpha c = \alpha t$, the results would be safe.

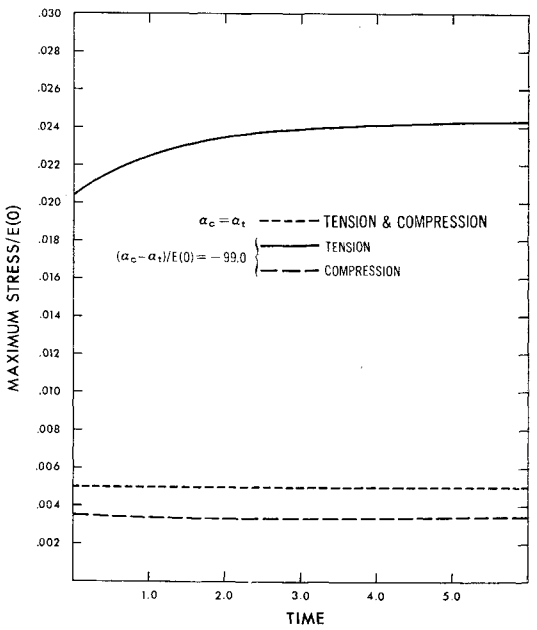

Fig. 3 Maximum stress vs time; $M/E(0) = 0.001$, $(\alpha_c - \alpha_t)/E(0) = -99.0$.

If, however, a constant moment is applied at $t = 0$, Eqs. (6) become harder to solve. To effect a solution for this case, the equations were finite-differenced and a Newton-Raphson scheme was used to solve them numerically. Figures 2 and 3 show the maximum stress in this case for two values of the parameters $(\alpha c - \alpha t)/E(0)$. Notice that in both cases, the maximum stress that is predicted by using $\alpha c = \alpha t$ is over 50% less than that predicted by the analysis when $\alpha c \neq \alpha t$.

In all figures, the following numerical values were used for the parameters:

$$b = 1,\ h = 1,\ \frac{E(t)}{E(0)} = 1 + e^{-t/\beta},\ \frac{M(t)}{E(0)} = 0.001$$

Conclusion

Although the results presented are for the simplest case that could be considered, there appear to be several safe generalizations one can make. The first is that the greater the difference in αt and αc, the more the actual stress will depart from that predicted by assuming that $\alpha c = \alpha t$. Also, for a given difference, the smaller $E(0)$, the greater the difference in stress for $\alpha c = \alpha t$ and $\alpha c \neq \alpha t$. Thus for materials with a relatively strong matrix, the error involved in using a standard analysis would not be too great. However, for materials with a weak matrix, a design based on the standard analysis could be grossly in error.

Computation of Axisymmetric Contractions

HARTMUT H. BOSSEL*
University of California, Santa Barbara, Calif.

Introduction

CONTRACTIONS, as in wind tunnels, must fulfill two basic requirements. First, the exit velocity at the narrow end must be uniform and parallel. Second, there must be no regions of separation caused by adverse pressure gradients at the wall which may appear at the start of the contraction and at the neck.

Many wind-tunnel contractions have been, and are being, designed by intuition. Unless model tests are made, the results are unpredictable and often unsatisfactory. It is clearly better to base the design on theoretical studies. Several methods for the design of axisymmetric contractions have been proposed over the years, unfortunately, all without experimental verification. In reviewing these methods for possible application to the design of a low-turbulence wind-tunnel contraction, it was found that none was entirely satisfactory. The method to be presented here is an outgrowth of these studies. It is a reformulation of Thwaites' solution[1] and has been found to be quick and convenient. An axisymmetric contraction with a 16/1 contraction ratio was designed using this method, built, and tested. The measured velocity distributions at entrance, exit, and on the wall will be presented and compared with the theoretical data.

Methods for the computation of axisymmetric potential flow fall into four broad categories: 1) adaptation of two-di-

Received January 13, 1969; revision received May 20, 1969. The author gratefully acknowledges the assistance of mechanical engineering students W. Sun, who built the contraction, L. Fafarman, who assembled the wind tunnel, and J. D. Riley, who carried out the measurements.

* Assistant Professor of Mechanical Engineering. Member AIAA.